HHS Public Access

Author manuscript

Anal Chem. Author manuscript; available in PMC 2024 March 21.

Published in final edited form as:

Anal Chem. 2023 March 21; 95(11): 4984–4991. doi:10.1021/acs.analchem.2c05222.

Investigating Daptomycin-Membrane Interactions Using Native MS and Fast Photochemical Oxidation of Peptides in Nanodiscs

Deseree J. Reid[1,†], **Tapasyatanu Dash**[1,†], **Zhihan Wang**[1], **Craig A. Aspinwall**[1,2], **Michael T. Marty**[1,2,*]

[1]Department of Chemistry and Biochemistry, University of Arizona, Tucson, AZ 85721, USA

[2]Bio5 Institute, University of Arizona, Tucson, AZ 85721, USA

Abstract

Daptomycin is a cyclic lipopeptide antibiotic that targets the lipid membrane of Gram-positive bacteria. Membrane fluidity and charge can affect daptomycin activity, but its mechanisms are poorly understood because it is challenging to study daptomycin interactions within lipid bilayers. Here, we combined native mass spectrometry (MS) and fast photochemical oxidation of peptides (FPOP) to study daptomycin-membrane interactions with different lipid bilayer nanodiscs. Native MS suggests that daptomycin incorporates randomly and does not prefer any specific oligomeric states when integrated into bilayers. FPOP reveals significant protection in most bilayer environments. Combining the native MS and FPOP results, we observed that stronger membrane interactions are formed with more rigid membranes, and pore formation may occur in more fluid membranes to expose daptomycin to FPOP oxidation. Electrophysiology measurements further supported the observation of polydisperse pore complexes from the mass spectrometry data. Together, these results demonstrate the complementarity of native MS, FPOP, and membrane conductance experiments to shed light on how antibiotic peptides interact with and within lipid membranes.

Graphical Abstract

[*]**Corresponding Author:** mtmarty@arizona.edu.
[†]These authors contributed equally.

ASSOCIATED CONTENT

Supporting Information. Supplemental methods for sample preparation and analysis; supplemental figures of native MS and FPOP tandem MS, and SCR data; and supplemental tables with lipid properties and mass defect values. This material is available free of charge via the Internet at http://pubs.acs.org.

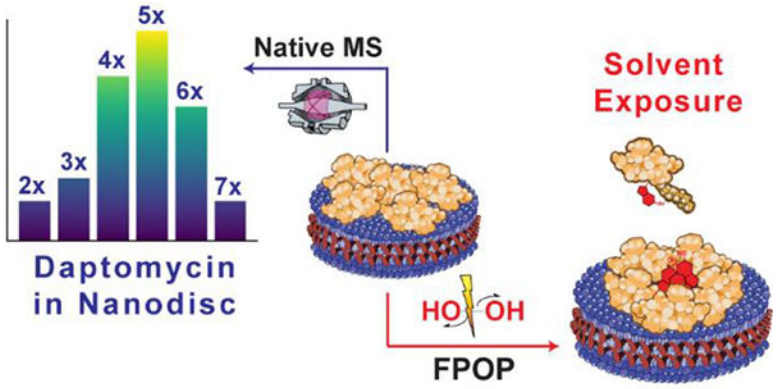

INTRODUCTION

Daptomycin is an FDA-approved antimicrobial peptide (AMP)[1] used intravenously to treat right-sided endocarditis and complicated skin and soft tissue infections that do not respond to first-line treatments.[2,3] It is listed by the World Health Organization as critically important for human medicine.[4] Daptomycin and other AMPs disrupt bacterial membranes by targeting their lipid bilayers directly, leading to cell death.[5] Although still uncommon, resistance against daptomycin has been observed recently.[6] Understanding its mechanism of action and resistance will help in the development of better therapies to combat the growing threat of antibiotic resistance.

However, it is challenging to study the polydisperse and dynamic interactions that daptomycin and other AMPs exhibit with lipid environments.[7] We have previously shown that intact AMP-nanodisc complexes can be analyzed via native mass spectrometry (MS) to determine the stoichiometry and the specificity of AMPs in different bilayers.[8–10] Native MS uses non-denaturing ionization conditions to preserve intact macromolecular complexes for mass analysis, including in intact nanodisc complexes.[11] However, native MS only informs on stoichiometries and is blind to the orientation of peptides within the nanodisc.

To complement native MS, we previously used fast photochemical oxidation of peptides (FPOP) in combination with liquid chromatography and mass spectrometry (LC-MS) to study AMP incorporation in nanodiscs with either synthetic or natural lipids.[12] FPOP is a footprinting technique that covalently and irreversibly labels solvent-accessible residues on proteins and peptides by generating hydroxyl radicals from hydrogen peroxide using a 248 nm KrF excimer laser.[13] Oxidative modifications to these species result in predictable mass shifts that are detected by MS. FPOP has been used to investigate a variety of proteins with model membrane systems such as nanodiscs,[12,14] micelles,[15] bicelles,[16] and even living organisms.[17] Other rapid footprinting chemistries have also been successfully used for membrane proteins, including the trifluoromethyl radical ($\cdot CF_3$), carbenes derived from diazirines, and carbocations.[18–25] Slower covalent labeling reagents, including glycine ethyl ester[26] diethylpyrocarbonate[27] have also proven effective. The field is rapidly advancing with the development of new reagents that differ in reactivities, kinetics, and selectivity

to enhance structural investigations of diverse targets. However, it remains challenging to interpret footprinting data for polydisperse complexes.

Here, we combined complementary native MS and FPOP experiments to study daptomycin interactions with different lipid nanodiscs to study its membrane interactions (Figure 1). We determined both the stoichiometries and oxidative labeling of daptomycin in different lipid environments. We chose lipids to test the effects of various lipid head groups and tails on daptomycin incorporation. Our results suggest that daptomycin interactions are somewhat affected by the lipid head group, but membrane fluidity and lipid tail interactions more significantly affect incorporation and orientation within membranes. We also show how native MS and FPOP can be combined to yield complementary information on membrane interactions.

EXPERIMENTAL SECTION

Reagents.

1,2-Dilauryl-*sn*-glycero-3-phosphocholine (DLPC), 1,2-dimyristoyl-*sn*-glycero-3-phosphocholine (DMPC), 1,2-dimyristoyl-*sn*-glycero-3-phospho-(1′-rac-glycerol) (DMPG), 1-palmitoyl-2-oleoyl-*sn*-glycero-3-phosphocholine (POPC), 1,2-dipalmitoyl-*sn*-glycero-3-phosphocholine (DPPC), and *E. coli* polar lipid extract lipids were purchased from Avanti Polar Lipids. Lipid structures and physical properties are provided for reference in Figure S1 and Table S1, respectively.

Daptomycin was purchased from Acros Organics. Additional reagent information is provided in the Supporting Information. Daptomycin stocks were prepared in 0.2 M ammonium acetate at 60 μM, 180 μM, and 360 μM and then diluted as described below for either native MS or FPOP analysis. No daptomycin aggregation was observed at any of the concentrations used. Calcium was present in daptomycin samples as an excipient from the manufacturer, and the calcium concentration was measured by ICP-MS as described in the Supplemental Methods.

Native MS Sample Preparation and Analysis.

Nanodiscs were prepared with DLPC, DMPG, DMPC, POPC, or DPPC as previously described[12, 28–31] and were mixed with daptomycin at 3:1, 9:1, or 18:1 daptomycin: nanodisc ratios for native MS analysis on a Q-Exactive HF UHMR as previously described.[8,9] Full details are provided in the Supplemental Methods.

FPOP.

Stock phosphate buffered saline (PBS) was prepared at 0.1 M. Stock H_2O_2 was prepared at ~200 mM in PBS. Glutamine stock was prepared at 0.20 M in PBS. Methionine stock was made at 0.19 M in PBS. Catalase stock was prepared at 4.2 μM in PBS. Nanodisc stocks were made at 20 μM. At room temperature, stock daptomycin was added to the nanodiscs at 3:1, 9:1, and 18:1 peptide: nanodisc ratios in the FPOP solution. Each ingredient was added separately in the order listed below for a final pre-FPOP solution volume of 50 μL.

Samples at a 3:1 daptomycin: nanodisc ratio were prepared as follows: 30 μL PBS (final concentration 80 mM), 5 μL glutamine (final 20 mM), 5 μL nanodiscs (final 2.0 μM), 5 μL 60 μM daptomycin (final 6.0 μM), and 5 μL H_2O_2 (final ~20 mM). 9:1 and 18:1 daptomycin: nanodisc samples were prepared similarly but with 5 μL of either 180 μM daptomycin (final 18.0 μM) or 360 μM daptomycin (final 36.0 μM), respectively. To minimize pre-FPOP oxidation, H_2O_2 was added immediately before laser irradiation.

Each sample was loaded into a Hamilton syringe and injected through the capillary using a syringe pump into the FPOP laser path. Instrumental details on the FPOP setup are provided in the Supplemental Methods. The samples were collected immediately after laser exposure into vials containing 11 μL of a mixture of 0.19 M methionine and 4.2 μM catalase to quench the remaining radicals. The final sample volume was 61 μL. After labeling, samples were analyzed by LC/MS as described in the Support Methods.

Daptomycin Electrophysiological Measurements.

Black lipid membranes (BLMs) were formed on pipettes as described previously[32] and in the Supplemental Methods. PBS was used as the recording bath buffer. To allow daptomycin reconstitution into the BLMs and to investigate the concentration dependence of daptomycin activities in the lipid membranes, three in-bath concentrations of daptomycin were prepared: 0.01, 0.1, and 1 mg/mL (6.17, 61.7, and 617 μM). Daptomycin PBS solution was perfused into the recording bath at the target concentrations and allowed to equilibrate for 15 minutes. Single channel recording (SCR) was then performed at a membrane potential of −70 mV. Membrane conductance was measured using a protocol previously described.[33]

RESULTS

Effects of Lipid Headgroup.

To investigate the effects of lipid headgroup on daptomycin incorporation into lipid bilayers, we first added daptomycin to lipid nanodiscs made with either DMPG or DMPC. DMPG is an anionic phosphatidyl-glycerol lipid with two saturated, 14-carbon tails. DMPC, its zwitterionic counterpart, has a phosphatidyl-choline headgroup and the same tails. Because daptomycin has a −3 charge at physiological pH, we predicted it would incorporate more in DMPC nanodiscs than in DMPG.

We first examined daptomycin added at a 9:1 daptomycin: nanodisc ratio. Native MS was used to determine the average number of incorporated daptomycin in each type of nanodisc. As predicted, more daptomycin was incorporated into DMPC than DMPG nanodiscs (shown isolated in Figure S2A and Figure 2A, *blue* and *black*). The anionic charge of the DMPG lipids likely hampers daptomycin incorporation due to charge repulsion.

Although daptomycin has a net −3 charge at neutral pH, the charge is reduced upon binding to divalent calcium ions. Thus, the interactions between the anionic PG lipids and daptomycin are commonly attributed to electrostatics when calcium is present.[34–38] The evidence for PG selectivity is further inferred from its higher abundance in susceptible strains and lower abundance in resistant and producer strains.[6,39] Most of these experiments were conducted on liposomes containing both PG and PC lipids, but prior studies have

demonstrated direct interactions with zwitterionic PC membranes in the presence of >1 mM calcium.[38,40]

Interestingly, some studies have observed minimal shifts in the intrinsic fluorescence emission spectrum of daptomycin in the presence of PC liposomes without calcium.[36,38] These data suggest that daptomycin does not bind PC membranes in the absence of calcium. In contrast, our experiments clearly detected binding with only background levels of calcium present. Although it is not clear if all background calcium was removed in prior studies, our best explanation of these contrasting data is that the micromolar background calcium levels present in our samples were enough to promote PC lipid binding. Future studies will explore the effect of calcium concentration in detail.

Examining the precise distribution of stoichiometries (Figure S3), we found that neither DMPG nor DMPC showed any convincing evidence for the formation of specific oligomeric complexes. As described previously,[8,9,10] formation of specific oligomeric complexes would create stoichiometry distributions with clear preferences. Instead, we observe roughly Poisson distributions, which indicates that no specific oligomers are preferred under these conditions. Ejected peptide-lipid aggregates were not observed in native MS spectra, even at higher collision energies, which is likely due to instrumental limitations in simultaneously analyzing large and small species.

To complement the native MS data, we performed FPOP under similar conditions to study changes in its solvent accessibility. Daptomycin inserts into bilayers via its N-terminal acyl tail,[35] so we expect that the peptide embeds this hydrophobic moiety into the bilayer, rather than only associated peripherally with head groups. An oxidizable tryptophan residue is close to this tail. MS/MS of oxidized FPOP confirmed that tryptophan is the primary oxidized species (Figure S4). When the second oxidized peak was isolated, some signals were observed for the oxidized cyclic portion of the molecule, likely at the kynurenine residue. Unfortunately, we could not further fragment the cyclic portion of daptomycin using CID, so oxidation of the kynurenine residue could not be conclusively verified. However, only the first oxidized peak was used in our analysis, so we can consider the global oxidation of the daptomycin as a proxy for tryptophan oxidation. Thus, we predicted that this tryptophan would be protected from oxidation upon daptomycin insertion into the nanodisc membrane.

Free daptomycin was readily oxidized and, importantly, did not show evidence for self-association in solution. Native MS revealed that it is monomeric and does not oligomerize in the absence of nanodiscs at all concentrations tested (Figure S5). The lack of solution phase oligomerization is further confirmed by FPOP measurements (Figure 3A), which show no significant changes in the oxidation of the free peptide with increasing concentration. These results agree with prior experiments that reported no daptomycin oligomers present in the solution at these concentrations.[35]

In contrast, at a 9:1 daptomycin: nanodisc ratio, daptomycin was significantly protected from oxidation. Similar levels of protection were observed in DMPG and DMPC nanodiscs (shown in Figure 3A and isolated in Figure S2B). The decreased oxidation indicates less

solvent exposure in both lipid environments relative to free in solution, despite significantly lower incorporation in DMPG nanodiscs observed by native MS (Figure 2 and S2A). As discussed below, these results may indicate that daptomycin only loosely associates with DMPG and that this loose incorporation is not native MS stable, resulting in the lower numbers of incorporation observed in native MS.

Effects of Daptomycin Concentration.

Next, we investigated the effects of daptomycin concentration on incorporation and solvent exposure. We added daptomycin to both DMPG and DMPC nanodiscs at 3:1 and 18:1 ratios and performed native MS and FPOP analysis. Higher ratios consistently increased the incorporation into nanodiscs during native MS (Figure 2B and Figure S2A). However, DMPC nanodiscs incorporation was always higher than DMPG at the same ratio. At all ratios, daptomycin formed no specific oligomeric complexes, neither in DMPG nor DMPC (Figure S3). We also calculated the percentage incorporation by dividing the average number of daptomycin incorporated per nanodisc by the total ratio of daptomycin added per nanodisc (Figure S6).

FPOP revealed the same levels of oxidation for both lipids at each ratio (Figure 3B and S2B) but increased oxidation at higher concentrations of 9:1 and 18:1. Free daptomycin oxidation did not change significantly with increasing concentration. The observed increase in oxidation suggests daptomycin is more solvent exposed at higher ratios, which contradicts the increases in percent membrane bound (Figure S6B). The presence of a pore within the bilayer would create a central region that is solvent accessible and may explain this observation if it exposes the oxidizable tryptophan residue (Figure 4). However, other conformational changes within the membrane or different partitioning between the membrane and solution could also affect solvent exposure, as discussed below.

Effects of Lipid Tails.

To investigate the effects of lipid tails on daptomycin incorporation, we performed the same experiments in nanodiscs composed of PC lipids with different tails: DLPC, DMPC, DPPC, and POPC. DLPC, DMPC, and DPPC are all saturated with 12:0, 14:0, and 16:0 tails, respectively. POPC is mixed with 16:0/18:1.

Native MS showed that daptomycin was generally most highly incorporated in DPPC, especially at higher ratios (Figure 2A). Incorporation was comparable for DMPC and POPC at every ratio. Incorporation in DLPC was generally lower than the other lipids, except at the lowest ratio. Similar trends were observed for percent incorporation (Figure S6). Because DPPC bilayers are the most rigid of the three PC types we investigated (Table S1), these results suggest that daptomycin incorporation and/or native MS stability is enhanced by lower membrane fluidity, which is discussed further below.

In contrast, FPOP oxidation of daptomycin in DPPC and DMPC nanodiscs did not show any statistically significant differences (Figure 3A). DLPC had slightly higher oxidation than DPPC at higher ratios. However, the largest differences were for POPC, which showed greater oxidation than all other lipids and was comparable with free daptomycin. Thus, in the presence of POPC nanodiscs, daptomycin is more solvent exposed than with any other

lipid nanodiscs. The missing protection in POPC may indicate a different orientation on the membrane, despite similar levels of incorporation with DMPC, as discussed below. For example, pore formation may expose residues to solvent despite being associated with the membrane.

Comparing the effects of increasing daptomycin concentration (Figure 3B), DMPC and DMPG were the only synthetic lipid environments where daptomycin had a significant increase in oxidation at higher ratios. As discussed, this increase in oxidation could indicate possible concentration-dependent pore formation. However, this trend is absent in POPC, DPPC, and DLPC, potentially because increased solvent exposure within the membrane may be canceled out by an overall increase in membrane association. In any case, the native MS and FPOP results reveal that lipid tails can affect the level of incorporation and solvent exposure for daptomycin in membranes.

Lastly, we investigated the effects of a mixed lipid environment on daptomycin incorporation. To test this, we used *E. coli* polar lipid extract to make nanodiscs and then performed FPOP. Although *E. coli* is Gram-negative, it contains a mixture of PE, PG, and cardiolipin lipids, which are also components of Gram-positive bacterial membranes. Because *E. coli* nanodiscs are polydisperse, their precise masses cannot be determined using traditional native MS, so only FPOP analysis was performed. FPOP revealed that the oxidation of daptomycin in *E. coli* nanodiscs is very similar to DLPC, DMPC, DMPG, and DPPC (Figure 3). Thus, daptomycin is similarly protected in the presence of DLPC, DMPC, DMPG, DPPC, and *E. coli* nanodiscs.

Only daptomycin in POPC showed major significant differences in oxidation from each of the other lipid types. POPC produces a very fluid bilayer, so increased bilayer fluidity may make the daptomycin more accessible to solvent. Supporting this observation, DLPC, the most fluid of the saturated lipids (Table S1), showed slightly higher oxidation than DPPC, the least fluid. However, DLPC, POPC, and *E. coli* lipids have similar phase transition temperatures (Table S1), so fluidity alone cannot account for these differences.

Conductance Measurements Reveal Daptomycin Pores.

Several trends in the FPOP data seem to point to daptomycin pore formation at higher concentrations. To test this proposed mechanism, we performed electrophysiology measurements using a black lipid membrane (BLM) prepared from POPC. Unfortunately, other lipid types were not amenable to the formation of stable BLMs under the experimental conditions. In the experimental single-channel recordings, stochastic step changes in current were observed over time (Figure 5A), which indicate changes in ion fluxes through the BLMs caused by the opening and closing of membrane pores. Changing ion conductance through pores could be due to dynamic conformational changes or to the transient formation and dissociation of daptomycin complexes in the membrane through diffusion.

At low concentrations, only very small current changes were observed (Figure 5A). However, at higher concentrations, two predominant step changes were observed to show step magnitudes of ~1.7 and ~4 pA. At the highest concentration, some additional step sizes were observed at much larger values. Such changes in step magnitude can be caused

by changes in pore conformation and stoichiometry, suggested by previous research of analogous pore-forming peptides.[27,41] Step size measurements were also supported by global measurements of membrane conductance. Here, the membrane conductance increased from ~0.01 nS to ~0.15 nS over increasing daptomycin concentration (Figure 5B).

These data demonstrate that daptomycin activities in lipid membranes are concentration dependent and that it does not form monodisperse pore complexes. Instead, higher daptomycin concentrations cause larger single-pore conductance. This larger conductance could be caused by conformational changes to a single oligomeric state that result in a larger pore (conformational polydispersity). However, the concentration dependence and native MS data suggest that the distribution in step sizes is caused by daptomycin complexes with different oligomeric states (oligomeric polydispersity) and thus different pore sizes. Overall, electrophysiological analysis suggests that daptomycin forms polydisperse, unorganized pores in POPC, which is consistent with the pore formation hypothesis proposed by FPOP data.

DISCUSSION

Overall, native MS revealed that daptomycin was incorporated the most in DPPC nanodiscs, followed by POPC and DMPC at equal levels, and finally the least in DMPG and DLPC (Figure 2). Across all lipid types, higher concentrations consistently lead to greater membrane incorporation (Figure 2B) but generally little to no change in the overall percentage of molecules incorporated (Figure S6B). Differences in incorporation between head groups could be explained by either the anionic charge of DMPG preventing incorporation due to charge repulsion or by weakly incorporated daptomycin that is not detectable via native MS.

Differences in incorporation between lipid tails are partially explained by their membrane fluidity. Because DPPC and POPC have similar thicknesses (Table S1) but different levels of daptomycin incorporation (Figure 2), these data indicate that membrane thickness cannot explain the data. During native MS, the ambient temperature of the needle with the solution was around 30 °C. At this temperature, DMPC and POPC are in their disordered fluid phase, but DPPC is in its ordered gel phase. DLPC experiments were performed at 15 °C to help preserve complex stability but are also well above their phase transition temperature and are thus in the disordered fluid phase. Contradicting some previous reports,[42,43] our data may thus indicate that daptomycin incorporates more strongly into rigid membranes, which may be because of its saturated lipid tail. Thus, low incorporation in DLPC nanodiscs is likely due to their increased fluidity rather than their decreased thickness.

As noted in the results above, solvent exposure data from FPOP contradicts the native MS results in several places. With FPOP, the highest oxidation and thus greatest solvent exposure was from free daptomycin and POPC nanodiscs, which were similar. DLPC, DMPC, DMPG, DPPC, and *E. coli* nanodiscs all had lower and similar oxidation. Because aggregation was not observed for daptomycin free in solution at any of the concentrations used, it is unlikely that changes in the free, unbound molecule contributed to the observed

differences in oxidation. There are several potential ways to interpret this contradictory data on membrane interactions.

One interpretation of the FPOP results is that they are primarily revealing global membrane association, with protection when bound to the membrane and constant oxidation when free in solution. Supporting this hypothesis, recent work from Sharp and coworkers suggests that micelles do not scavenge hydroxyl radicals from bulk solution but protect molecules close to the micelle surface, even seemingly solvent-exposed moieties.[44] If this were the case, clear differences in native MS incorporation for DLPC, DMPG, DMPC, and DPPC—despite similar FPOP oxidation—would indicate different types of membrane interactions that are more or less stable during native MS. Daptomycin may only weakly associate with DLPC and DMPG nanodiscs and thus easily fall off during native MS. In contrast, daptomycin could strongly integrate into DPPC nanodiscs and better survive the transfer into the mass spectrometer. Both cases would have similar protection by FPOP. Here, FPOP would be only sampling the equilibrium between oxidized free peptide and protected membrane-bound peptide.

However, results from POPC reveal that this interpretation is at least incomplete. Through this lens, FPOP would indicate no incorporation into POPC nanodiscs, but the native MS data clearly demonstrates association with the membrane. Therefore, it must be possible for daptomycin to incorporate with the nanodiscs in a way that is susceptible to FPOP oxidation yet detectable by native MS.

To inform our discussion, we considered the two data sets together and compared the observed oxidation to the theoretical oxidation predicted from a simple model of complete membrane protection. We assumed that nanodisc-incorporated daptomycin would be fully protected (0% oxidized) and that unincorporated daptomycin would be free in solution and oxidize at the same level as the mean oxidation of free daptomycin without nanodiscs (45% oxidized). We then calculated the theoretical oxidation by multiplying the fraction unbound (Figure S6) by 45%. Finally, we calculated the difference between the theoretical oxidation and the observed oxidation (Figure 6A).

This approach reveals two trends in the combined data (Figure 6). Negative values for oxidation difference indicate that the predicted oxidation was greater than the observed oxidation, meaning greater protection was observed by FPOP than expected by native MS. Here, DMPG and DLPC showed the greatest excess protection. Lesser but still significant values were observed with DMPC, especially at a 3:1 ratio. As described above, we believe these negative values likely indicate the presence of transient or weak interactions (especially with DPLC and DMPG) that are sufficient to protect daptomycin from oxidation in solution but fall apart during native MS (Figure 6B). Interestingly, both DMPG and DMPC deviations decrease at higher concentrations. The decreased deviation (Figure 6A) and increased percent associated (Figure S6) suggest a tighter association with the membrane at elevated concentrations, but we cannot rule out less protection in the membrane at higher ratios from pore formation or other conformational changes.

Conversely, positive values indicate that the observed oxidation was greater than the predicted oxidation, which means daptomycin was not perfectly protected from FPOP oxidation in the membrane compared to the incorporation percentage observed during native MS. POPC was the only lipid in which the observed oxidation was greater than the predicted oxidation (Figure 6A). The increased membrane fluidity of POPC may leave incorporated daptomycin more exposed, but it may also point to pore formation, which would potentially form complexes that expose the tryptophan residues to solvent (Figures 4 and 6C). Electrophysiology studies described above support the formation of polydisperse pore complexes in POPC membranes. Finally, both native MS and FPOP revealed that daptomycin was incorporated strongly into DPPC membranes at all concentrations, and DPPC was mostly consistent with the predicted values.

By combining data on incorporation stoichiometries from native MS, solvent exposure from FPOP, and membrane conductance by electrophysiology, our data begin to paint a picture of daptomycin interactions inside membranes. These results suggest that daptomycin likely forms transient and polydisperse, unorganized pore complexes that contain a range of different oligomeric states. These complexes are affected by both lipid head groups and lipid tails, which significantly affect both the overall affinity of daptomycin for lipid bilayers and the solvent exposure of the molecule when associated with membranes.

CONCLUSION

Here, we investigated the interactions of daptomycin with a variety of lipid nanodiscs using native MS and FPOP. Native MS revealed that daptomycin does not prefer any specific oligomeric states when incorporated into bilayers. Incorporation was lower in the anionic DMPG nanodiscs than in all other PC containing bilayers except DLPC, likely indicating that daptomycin interacts more weakly with DMPG under these conditions and thus does not survive the transfer into the mass spectrometer. FPOP revealed protection from oxidation upon incorporation into bilayers with greater membrane rigidity. Conversely, little protection was observed when daptomycin was incorporated into POPC nanodiscs. When both native MS and FPOP data are considered together, higher than expected solvent exposure in POPC membrane may indicate the formation of pores in these fluid membranes, which is supported by electrophysiology data.

Together, these results show the complementarity of native MS and FPOP experiments. FPOP revealed membrane association of daptomycin in DMPG and DLPC nanodiscs that did not survive native MS analysis. Conversely, native MS results clearly showed incorporation in POPC nanodiscs that was not reflected in the FPOP data. Thus, FPOP does not always simply report on global membrane association but can report on solvent exposure of specific residues on peptides at the membrane surface.

Future work will investigate daptomycin incorporation with carefully controlled concentrations of Ca^{2+}, which is implicated in daptomycin activity.[42,45,46] Future research will also expand upon these experiments to include nanodiscs composed of lipids from daptomycin-resistant bacteria. By comparing the behavior of daptomycin in nanodiscs

composed of lipids from resistant bacteria to those of susceptible bacteria, we hope to better understand how lipids modulate daptomycin activity.

Supplementary Material

Refer to Web version on PubMed Central for supplementary material.

ACKNOWLEDGMENT

The analysis for calcium concentration in daptomycin was performed by Mary Kay Amistadi in the Arizona Laboratory for Emerging Contaminants at the University of Arizona, Tucson, AZ. The pMSP1D1 plasmid was a gift from Stephen Sligar (Addgene plasmid #20061). This work was funded by the National Institutes of Health (R35 GM128624) and National Science Foundation (CBET-2003297). The content is solely the responsibility of the authors and does not necessarily represent the official views of the National Institutes of Health or the National Science Foundation.

REFERENCES

(1). Chen CH; Lu TK Development and Challenges of Antimicrobial Peptides for Therapeutic Applications. Antibiotics 2020, 9 (1), 24. 10.3390/antibiotics9010024. [PubMed: 31941022]

(2). Hamed K; Gonzalez-Ruiz A; Seaton A Daptomycin: An Evidence-Based Review of Its Role in the Treatment of Gram-Positive Infections. Infect Drug Resist 2016, 47. 10.2147/idr.s99046.

(3). Sauermann R; Rothenburger M; Graninger W; Joukhadar C Daptomycin: A Review 4 Years after First Approval. Pharmacology 2007, 81 (2), 79–91. 10.1159/000109868. [PubMed: 17940348]

(4). Critically important antimicrobials for human medicine, 6th revision. Geneva: World Health Organization; 2019

(5). Sani MA; Separovic F How Membrane-Active Peptides Get into Lipid Membranes. Acc Chem Res 2016, 49 (6), 1130–1138. 10.1021/acs.accounts.6b00074. [PubMed: 27187572]

(6). Miller WR; Bayer AS; Arias CA Mechanism of Action and Resistance to Daptomycin in Staphylococcus Aureus and Enterococci. Cold Spring Harb Perspect Med 2016, 6 (11). 10.1101/cshperspect.a026997.

(7). Liu XR; Zhang MM; Gross ML Mass Spectrometry-Based Protein Footprinting for Higher-Order Structure Analysis: Fundamentals and Applications. Chem Rev 2020, 120 (10), 4355–4454. 10.1021/acs.chemrev.9b00815. [PubMed: 32319757]

(8). Walker LR; Marty MT Revealing the Specificity of a Range of Antimicrobial Peptides in Lipid Nanodiscs by Native Mass Spectrometry. Biochemistry 2020, 59 (23), 2135–2142. 10.1021/acs.biochem.0c00335. [PubMed: 32452672]

(9). Walker LR; Marzluff EM; Townsend JA; Resager WC; Marty MT Native Mass Spectrometry of Antimicrobial Peptides in Lipid Nanodiscs Elucidates Complex Assembly. Anal Chem 2019, 91 (14), 9284–9291. 10.1021/acs.analchem.9b02261. [PubMed: 31251560]

(10). Walker LR; Marty MT Lipid Tails Modulate Antimicrobial Peptide Membrane Incorporation and Activity. Biochim Biophys Acta Biomembr 2022, 1864 (4). 10.1016/j.bbamem.2022.183870.

(11). Keener JE; Zhang G; Marty MT Native Mass Spectrometry of Membrane Proteins. Anal Chem. 2021, 93 (1) 583–597. 10.1021/acs.analchem.0c04342. [PubMed: 33115234]

(12). Reid DJ; Rohrbough JG; Kostelic MM; Marty MT Investigating Antimicrobial Peptide–Membrane Interactions Using Fast Photochemical Oxidation of Peptides in Nanodiscs. J Am Soc Mass Spectrom 2022, 33 (1), 62–67. 10.1021/jasms.1c00252. [PubMed: 34866389]

(13). Hambly DM; Gross ML Laser Flash Photolysis of Hydrogen Peroxide to Oxidize Protein Solvent-Accessible Residues on the Microsecond Timescale. J Am Soc Mass Spectrom 2005, 16 (12), 2057–2063. 10.1016/j.jasms.2005.09.008. [PubMed: 16263307]

(14). Lu Y; Zhang H; Niedzwiedzki DM; Jiang J; Blankenship RE; Gross ML Fast Photochemical Oxidation of Proteins Maps the Topology of Intrinsic Membrane Proteins: Light-Harvesting Complex 2 in a Nanodisc. Anal Chem 2016, 88 (17), 8827–8834. 10.1021/acs.analchem.6b01945. [PubMed: 27500903]

(15). Pan Y; Ruan X; Valvano MA; Konermann L Validation of Membrane Protein Topology Models by Oxidative Labeling and Mass Spectrometry. J Am Soc Mass Spectrom 2012, 23 (5), 889–898. 10.1007/s13361-012-0342-x. [PubMed: 22410873]

(16). Pan Y; Brown L; Konermann L Kinetic Folding Mechanism of an Integral Membrane Protein Examined by Pulsed Oxidative Labeling and Mass Spectrometry. J Mol Biol 2011, 410 (1), 146–158. 10.1016/j.jmb.2011.04.074. [PubMed: 21570983]

(17). Espino JA; Zhang Z; Jones LM Chemical Penetration Enhancers Increase Hydrogen Peroxide Uptake in C. Elegans for in Vivo Fast Photochemical Oxidation of Proteins. J Proteome Res 2020, 19 (9), 3708–3715. 10.1021/acs.jproteome.0c00245. [PubMed: 32506919]

(18). Oldham NJ Carbene Footprinting Reveals Binding Interfaces of a Multimeric Membrane-Spanning Protein. Angew Chem Int Ed Engl 2017, 56 (47), 14873–14877. DOI: 10.1002/anie.201708254. [PubMed: 28960650]

(19). Sun J; Liu XR; Li S; He P; Li W; Gross ML Nanoparticles and photochemistry for native-like transmembrane protein footprinting. Nat Commun 2021, 12 (1), 7270. DOI: 10.1038/s41467-021-27588-8. [PubMed: 34907205]

(20). Sun J; Li S; Li W; Gross ML Carbocation Footprinting of Soluble and Transmembrane Proteins. Anal Chem 2021, 93 (39), 13101–13105. DOI: 10.1021/acs.analchem.1c03274. [PubMed: 34558889]

(21). Cheng M; Guo C; Li W; Gross ML Free-Radical Membrane Protein Footprinting by Photolysis of Perfluoroisopropyl Iodide Partitioned to Detergent Micelle by Sonication. Angew Chem Int Ed Engl 2021, 60 (16), 8867–8873. DOI: 10.1002/anie.202014096. [PubMed: 33751812]

(22). Zhou F; Yang Y; Chemuru S; Cui W; Liu S; Gross M; Li W Footprinting Mass Spectrometry of Membrane Proteins: Ferroportin Reconstituted in Saposin A Picodiscs. Anal Chem 2021, 93 (33), 11370–11378. DOI: 10.1021/acs.analchem.1c02325. [PubMed: 34383472]

(23). Guo C; Cheng M; Li W; Gross ML Diethylpyrocarbonate Footprints a Membrane Protein in Micelles. J Am Soc Mass Spectrom 2021, 32 (11), 2636–2643. DOI: 10.1021/jasms.1c00172. [PubMed: 34664961]

(24). Pan X; Vachet RW Membrane Protein Structures and Interactions from Covalent Labeling Coupled with Mass Spectrometry. Mass Spectrom Rev 2022, 41 (1), 51–69. DOI: 10.1002/mas.21667. [PubMed: 33145813]

(25). Pan X; Tran T; Kirsch ZJ; Thompson LK; Vachet RW Diethylpyrocarbonate-Based Covalent Labeling Mass Spectrometry of Protein Interactions in a Membrane Complex System. J Am Soc Mass Spectrom 2023, 34 (1), 82–91. DOI: 10.1021/jasms.2c00262. [PubMed: 36475668]

(26). Dutton A; Singer SJ Crosslinking and Labeling of Membrane Proteins by Transglutaminase-Catalyzed Reactions (Membrane Structure/Fluorescent Probes) Proc Nat Acad Sci 1975, 72, (7), 2568–2571. 10.1073/pnas.72.7.2568 [PubMed: 241075]

(27). Bechinger B Structure and Functions of Channel-Forming Peptides: Magainins, Cecropins, Melittin and Alamethicin. J Membrane Biol 1997, 156, 197–211. 10.1007/s002329900201 [PubMed: 9096062]

(28). Kostelic MM; Zak CK; Liu Y; Chen VS; Wu Z; Sivinski J; Chapman E; Marty MT UniDecCD: Deconvolution of Charge Detection-Mass Spectrometry Data. Anal Chem 2021, 93 (44), 14722–14729. 10.1021/acs.analchem.1c03181. [PubMed: 34705424]

(29). Reid DJ; Keener JE; Wheeler AP; Zambrano DE; Diesing JM; Reinhardt-Szyba M; Makarov A; Marty MT Engineering Nanodisc Scaffold Proteins for Native Mass Spectrometry. Anal Chem 2017, 89 (21), 11189–11192. 10.1021/acs.analchem.7b03569. [PubMed: 29048874]

(30). Denisov IG; Grinkova Y. v.; Lazarides AA; Sligar SG Directed Self-Assembly of Monodisperse Phospholipid Bilayer Nanodiscs with Controlled Size. J Am Chem Soc 2004, 126 (11), 3477–3487. 10.1021/ja0393574. [PubMed: 15025475]

(31). Kostelic MM; Zak CK; Jayasekera HS; Marty MT Assembly of Model Membrane Nanodiscs for Native Mass Spectrometry. Anal Chem 2021, 93 (14), 5972–5979. 10.1021/acs.analchem.1c00735. [PubMed: 33797873]

(32). Bright LK; Baker CA; Agasid MT; Ma L; Aspinwall CA Decreased Aperture Surface Energy Enhances Electrical, Mechanical, and Temporal Stability of Suspended Lipid Membranes. ACS Appl Mater Interfaces 2013, 5 (22), 11918–11926. 10.1021/am403605h. [PubMed: 24187929]

(33). Agasid MT; Comi TJ; Saavedra SS; Aspinwall CA Enhanced Temporal Resolution with Ion Channel-Functionalized Sensors Using a Conductance-Based Measurement Protocol. Anal Chem 2017, 89 (2), 1315–1322. 10.1021/acs.analchem.6b04226. [PubMed: 27981836]

(34). Gray DA; Wenzel M More than a Pore: A Current Perspective on the in Vivo Mode of Action of the Lipopeptide Antibiotic Daptomycin. Antibiotics 2020, 9 (1), 17. 10.3390/antibiotics9010017. [PubMed: 31947747]

(35). Muraih JK; Pearson A; Silverman J; Palmer M Oligomerization of Daptomycin on Membranes. Biochim Biophys Acta Biomembr 2011, 1808 (4), 1154–1160. 10.1016/j.bbamem.2011.01.001.

(36). Ly WK; Cottagnoud P Daptomycin: A New Treatment for Insidious Infections Due to Gram-Positive Pathogens. Swiss Med Wkly 2008, 138(7–8), 93–9. 10.4414/smw.2008.12045. [PubMed: 18293118]

(37). Taylor R; Butt K; Scott B; Zhang T; Muraih JK; Mintzer E; Taylor S; Palmer M Two Successive Calcium-Dependent Transitions Mediate Membrane Binding and Oligomerization of Daptomycin and the Related Antibiotic A54145. Biochim Biophys Acta Biomembr 2016, 1858 (9), 1999–2005. 10.1016/j.bbamem.2016.05.020.

(38). Jung D; Rozek A; Okon M; Hancock REW Structural Transitions as Determinants of the Action of the Calcium-Dependent Antibiotic Daptomycin. Chem Biol 2004, 11, 949–957. 10.1016/j.chembiol.2004.04.020 [PubMed: 15271353]

(39). Hachmann AB; Sevim E; Gaballa A; Popham DL; Antelmann H; Helmann JD Reduction in Membrane Phosphatidylglycerol Content Leads to Daptomycin Resistance in Bacillus Subtilis. Antimicrob Agents Chemother 2011, 55 (9), 4326–4337. 10.1128/AAC.01819-10. [PubMed: 21709092]

(40). Chen YF; Sun TL; Sun Y; Huang HW Interaction of Daptomycin with Lipid Bilayers: A Lipid Extracting Effect. Biochemistry 2014, 53 (33), 5384–5392. 10.1021/bi500779g. [PubMed: 25093761]

(41). Heitz BA; Jones IW; Hall HK Jr.; Aspinwall CA; Saavedra SS Fractional Polymerization of a Suspended Planar Bilayer Creates a Fluid, Highly Stable Membrane for Ion Channel Recordings. J Am Chem Soc 2010, 132 (20), 7086–7093 10.1021/ja100245d [PubMed: 20441163]

(42). Pokorny A; Almeida PF The Antibiotic Peptide Daptomycin Functions by Reorganizing the Membrane. J Membr Biol 2021, 254 (1), 97–108. 10.1007/s00232-021-00175-0. [PubMed: 33620544]

(43). Boudjemaa R; Cabriel C; Dubois-Brissonnet F; Bourg N; Dupuis G; Gruss A; Lévêque-Fort S; Briandet R; Fontaine-Aupart MP; Steenkeste K Impact of Bacterial Membrane Fatty Acid Composition on the Failure of Daptomycin to Kill Staphylococcus Aureus. Antimicrob Agents Chemother 2018, 62 (7). 10.1128/AAC.00023-18.

(44). Cheng Z; Mobley C; Misra SK; Gadepalli RS; Hammond RI; Brown LS; Rimoldi JM; Sharp JS Self-Organized Amphiphiles Are Poor Hydroxyl Radical Scavengers in Fast Photochemical Oxidation of Proteins Experiments. J Am Soc Mass Spectrom 2021, 32 (5), 1155–1161. 10.1021/jasms.0c00457. [PubMed: 33881849]

(45). Beriashvili D; Taylor R; Kralt B; Abu Mazen N; Taylor SD; Palmer M Mechanistic Studies on the Effect of Membrane Lipid Acyl Chain Composition on Daptomycin Pore Formation. Chem Phys Lipids 2018, 216, 73–79. 10.1016/j.chemphyslip.2018.09.015. [PubMed: 30278162]

(46). Kreutzberger MA; Pokorny A; Almeida PF Daptomycin-Phosphatidylglycerol Domains in Lipid Membranes. Langmuir 2017, 33 (47), 13669–13679. 10.1021/acs.langmuir.7b01841. [PubMed: 29130685]

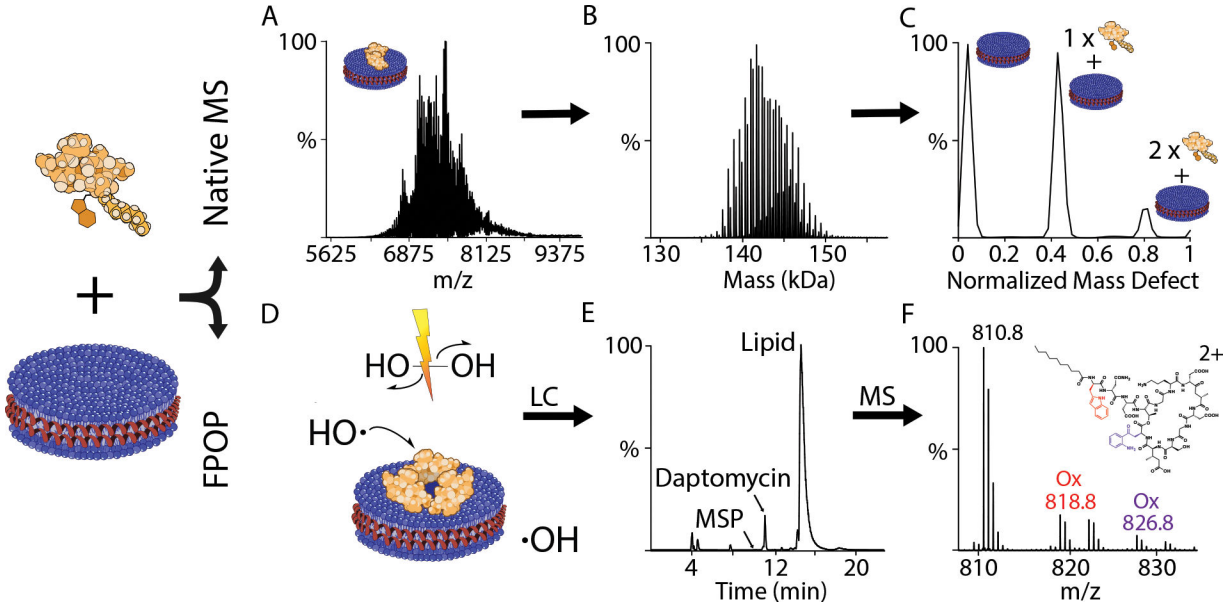

Figure 1.

Daptomycin is mixed with nanodiscs and then analyzed with native MS (A–C) and FPOP (D–F). The native *m/z* spectrum (A) is deconvolved into the zero-charge mass spectrum (B). Finally, mass defect analysis (C) is used to identify the number of daptomycin molecules incorporated. In FPOP, a UV laser produces hydroxyl radicals through photolysis, which label solvent accessible residues of daptomycin (D). Next, the solution is separated by LC (E), and oxidized peaks are quantified by MS (F).

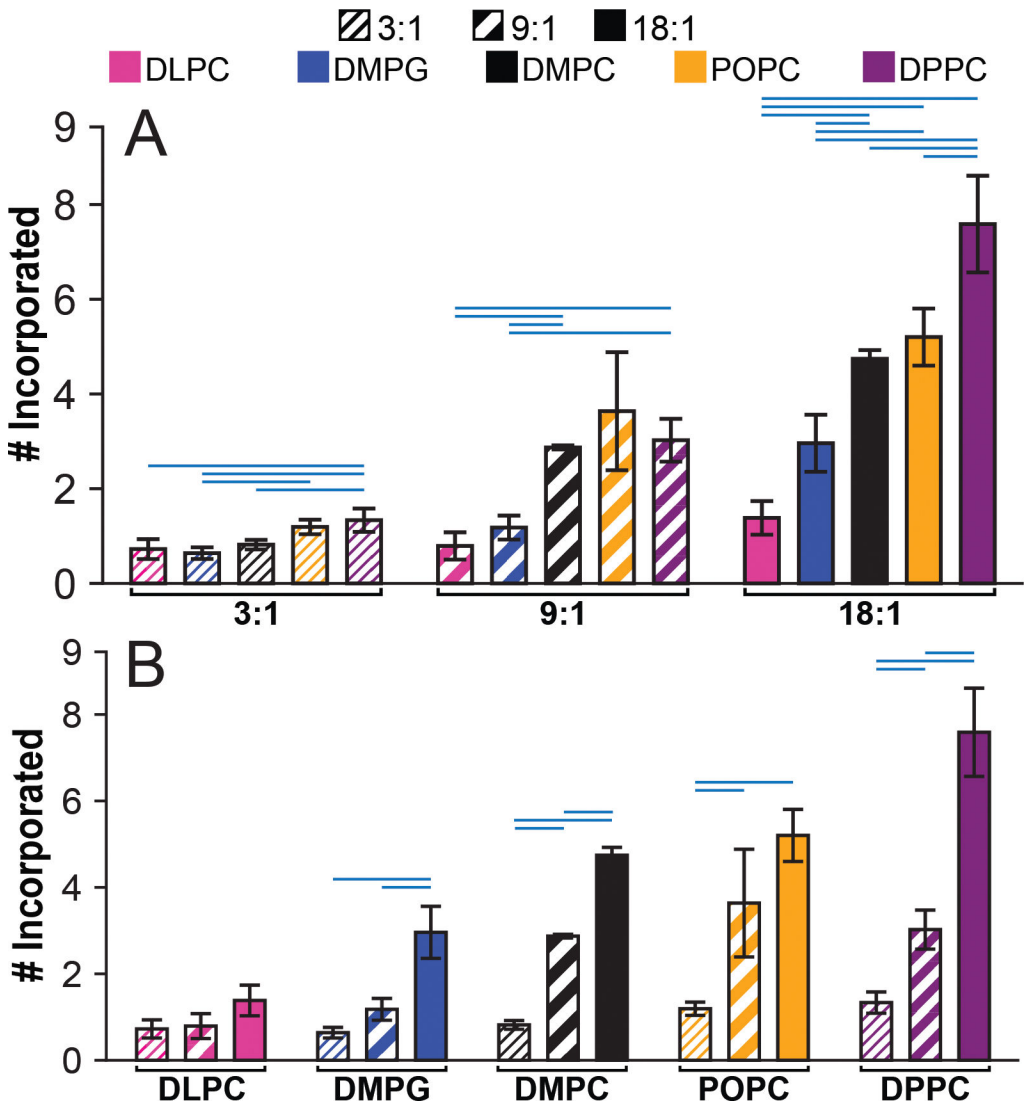

Figure 2.

Average number of incorporated daptomycin measured by native MS, grouped by (A) ratio or (B) lipid type with DLPC (*pink*), DMPG (*blue*), DMPC (*black*), POPC (*yellow*), and DPPC (*purple*) nanodiscs at 3:1 (*light shading*), 9:1 (*heavy shading*), and 18:1 (*solid*) daptomycin:nanodisc ratios. Horizontal blue bars that indicate statistically significant differences between pairs of measurements ($p < 0.05$). Error bars show standard deviations from replicate nanodiscs.

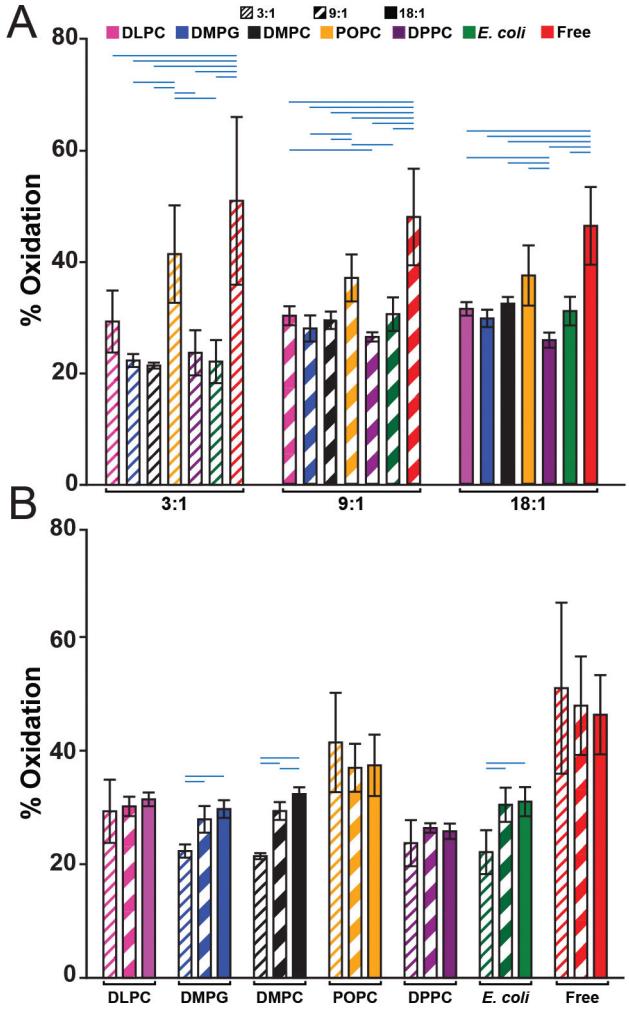

Figure 3.

FPOP oxidation of daptomycin grouped by (A) ratio or (B) lipid type with DLPC (*pink*), DMPG (*blue*), DMPC (*black*), POPC (*yellow*), DPPC (*purple*), and *E. coli* (*green*) nanodiscs and free daptomycin (*red*) at 3:1 (*light shading*), 9:1 (*heavy shading*), and 18:1 (*solid*) daptomycin:nanodisc ratios. Error bars indicate standard deviations. Horizontal blue bars that indicate statistically significant differences between pairs of measurements ($p < 0.05$).

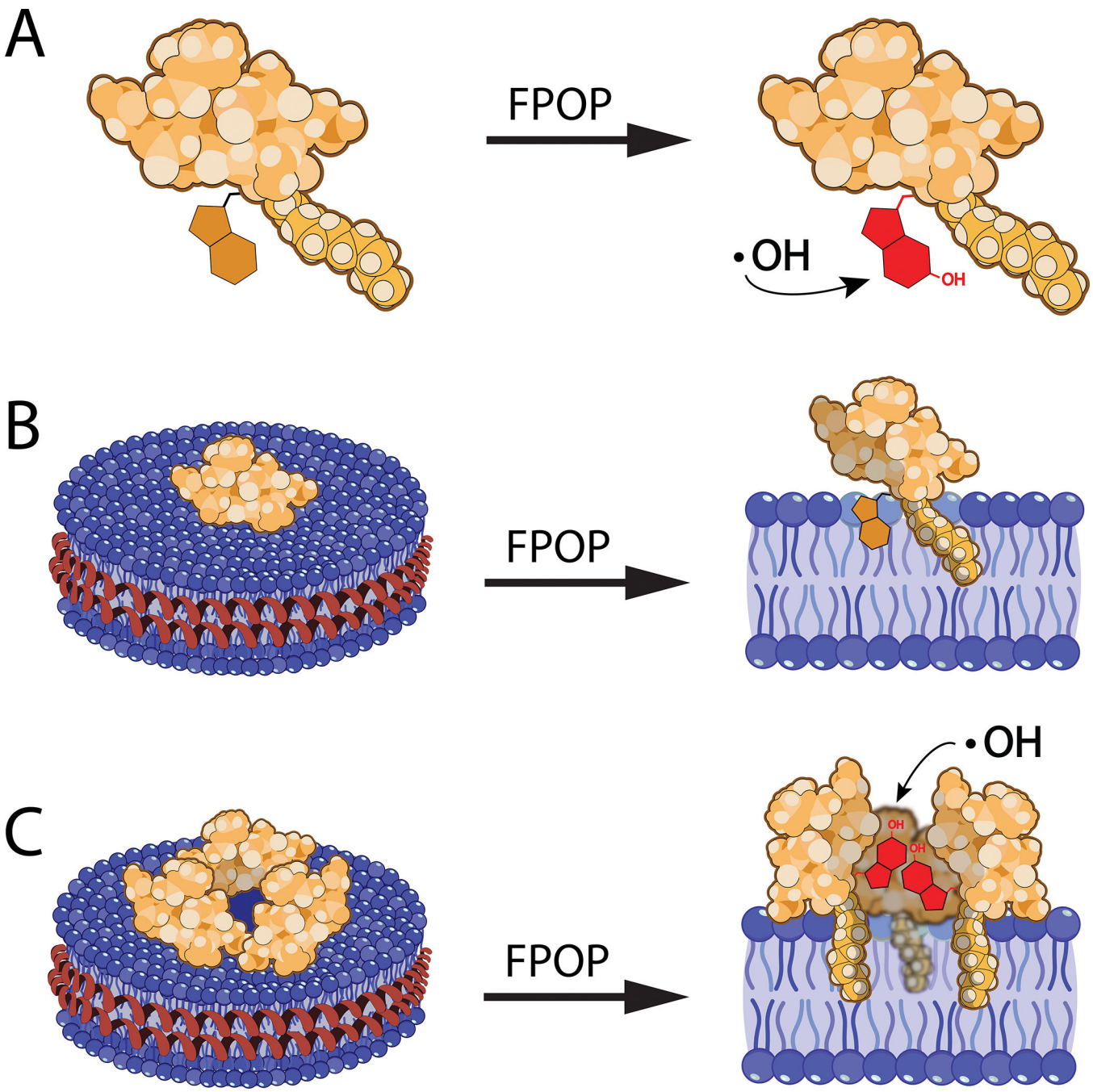

Figure 4.

Potential mechanisms of daptomycin incorporation into nanodiscs. Daptomycin is largely monomeric in solution at pH 7 and has an accessible tryptophan residue, which is readily oxidized (A). At low concentrations, the acyl tail of daptomycin inserts into the bilayer, protecting the tryptophan from oxidation (B). At higher concentrations, pore formation may occur, partially exposing tryptophan residues to the solvent and permitting oxidation (C).

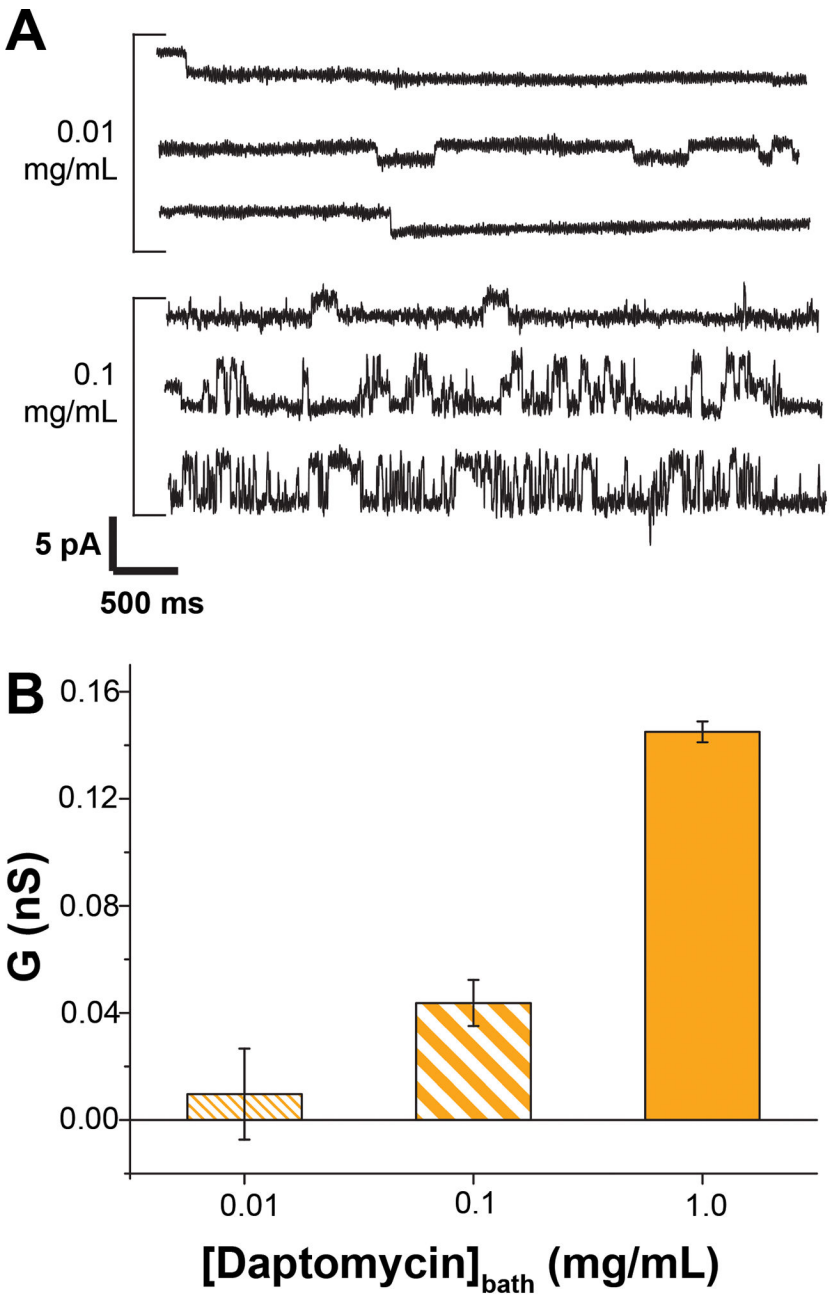

Figure 5.

(A) Representative single channel recording traces of daptomycin at in-bath concentrations 0.01 and 0.1 mg/mL. (B) Membrane conductance following daptomycin reconstitution at bath concentrations of 0.01 (*light shading*), 0.1 (*heavy shading*), and 1 (*solid*) mg/mL ($n = 3$) daptomycin.

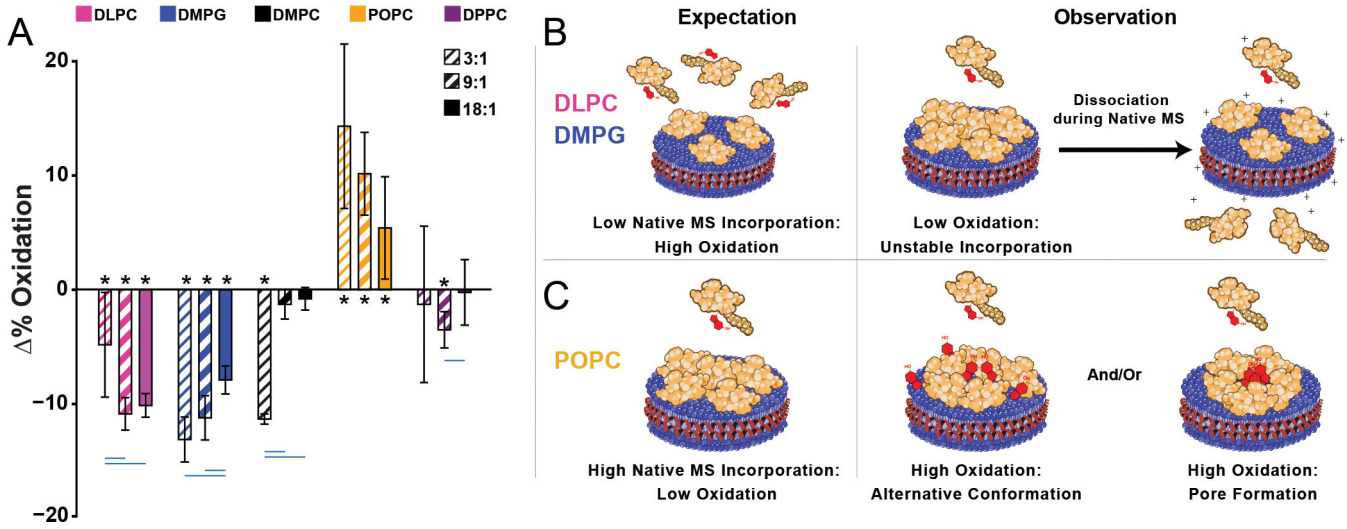

Figure 6.

A) The difference between the predicted oxidation based on the incorporation observed by native MS (assuming the average free daptomycin oxidation in solution and no oxidation inside the nanodisc) and the oxidation observed during FPOP is calculated for DLPC (*pink*), DMPG (*blue*), DMPC (*black*), DPPC (*purple*), and POPC (*yellow*) as described in the text. Negative values indicate more protection than expected based on native MS results. Positive values indicate less protection than expected. Vertical bars are 95% confidence intervals. Asterisks indicate confidence intervals that are statistically different from 0. Horizontal blue bars indicate statistically significant differences between pairs of measurements ($p < 0.05$). B) Schematic interpretation of the results. Negative values indicate more protection during FPOP than would be predicted by native MS, meaning that weak complexes potentially dissociated during native MS. C) Positive values indicate greater native MS incorporation than would be predicted by FPOP, which means daptomycin was not perfectly protected from FPOP oxidation in the membrane.